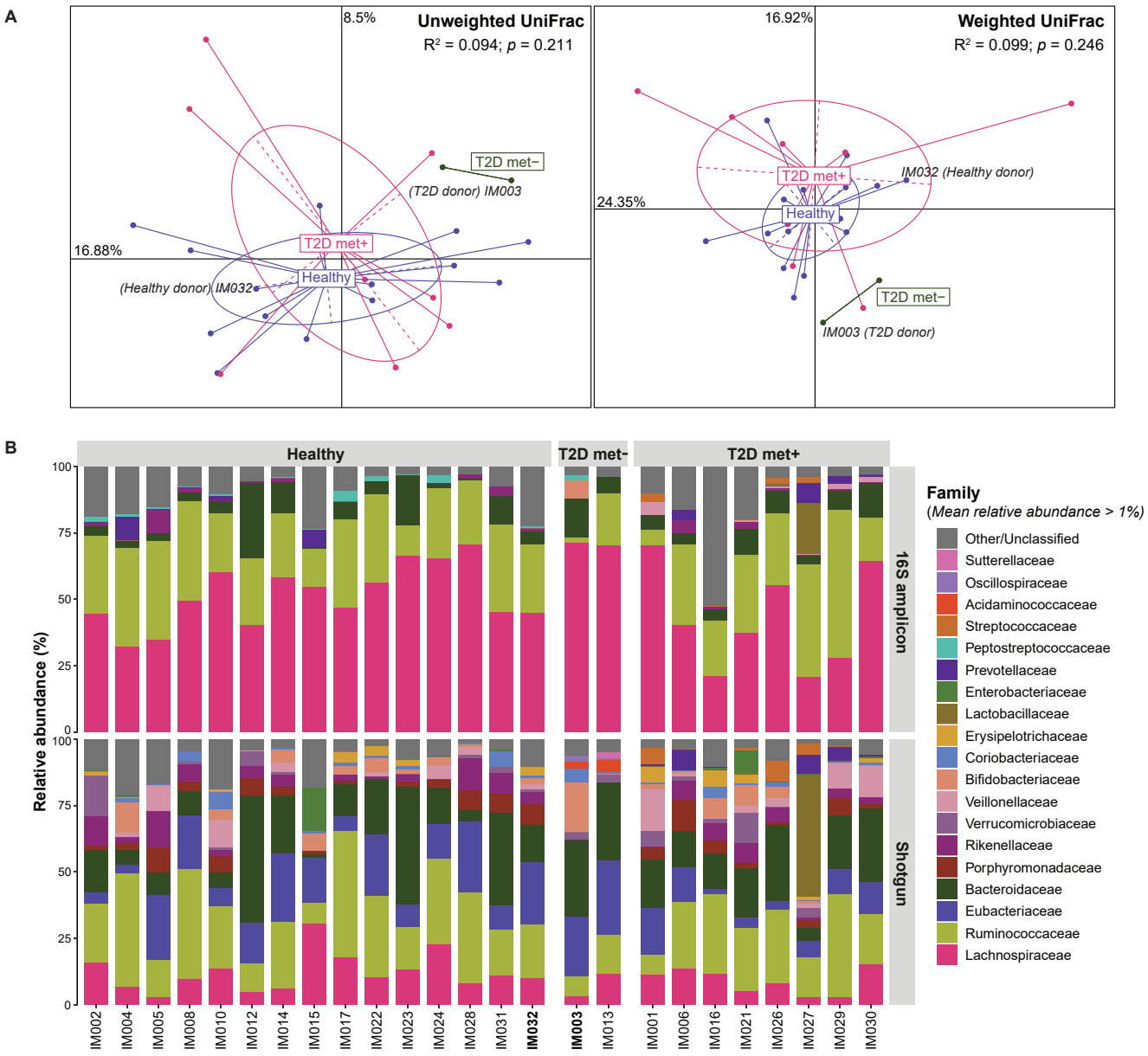

Figure S1. The taxonomic composition and the functional pathways encoded by the human gut microbiome donors align with diabetes status and metformin treatment. (**A**) Principle coordinates analysis plots based on unweighted and weighted UniFrac distances grouped by type 2 diabetes and metformin treatment. The significant differences between groups were calculated by permutational multivariate analysis of variance (PERMANOVA) tests. (**B**) The gut microbiota composition of obese adults with type 2 diabetes versus healthy were characterized by 16S rRNA gene amplicon sequencing and shotgun metagenomics. All known bacterial taxa with mean relative abundance less than 1% and unclassified taxa were merged to form the Other/Unclassified group.

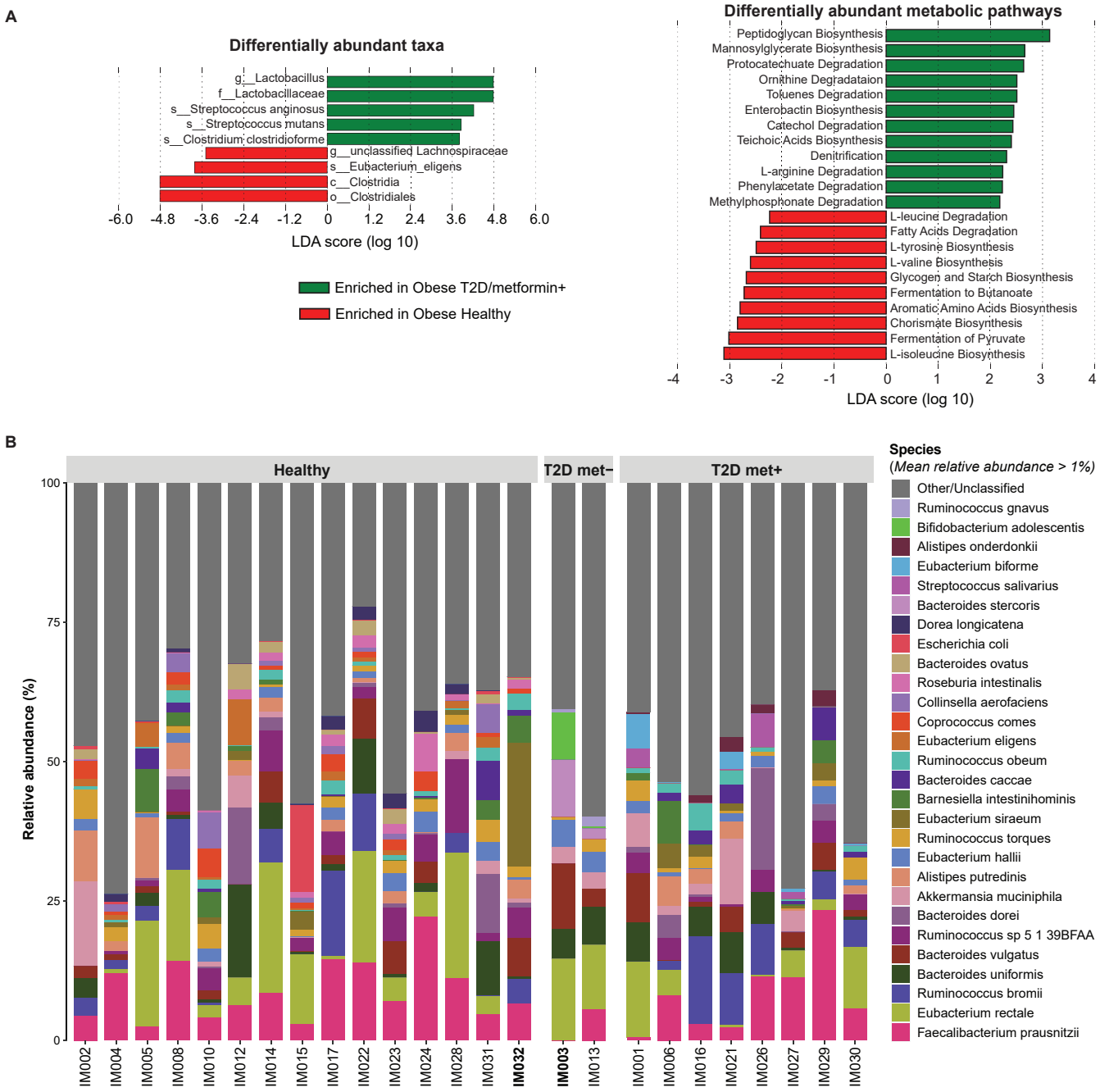

Figure S2. The taxonomic composition and the functional pathways of shotgun metagenomics encoded by the human gut microbiome donors align with diabetes status and metformin treatment. (**A**) Significantly differentially abundant bacterial taxa and functional pathways of shotgun data were identified by Linear Discriminant Analysis Effect Size (LEfSe) analysis ($p \leq 0.05$, Mann–Whitney U test; and LDA score > 2.0). (**B**) The gut microbiota composition of obese adults with type 2 diabetes versus healthy at species level. All known bacterial taxa with mean relative abundance less than 1% and unclassified taxa were merged to form the Other/Unclassified group. IM032 and IM003 were selected as donors for the human-to-mouse microbiome transplantation.

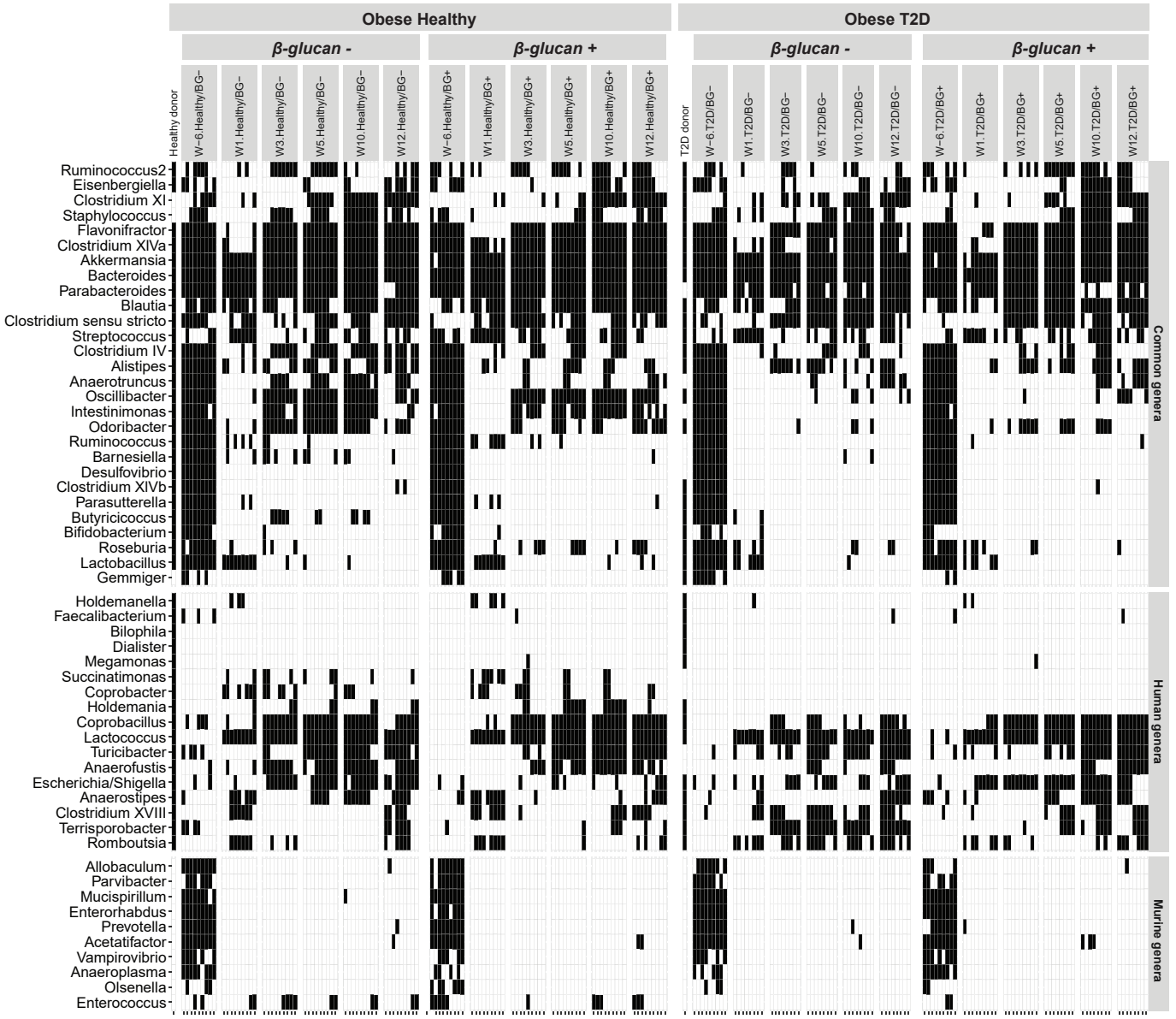

Figure S3. Engraftment of the two human gut microbiota donors into antibiotic-treated mice. Each column represents an individual and were organized according to donor type, diet and time point. Presence of genera is in black and absence as white. Only classified genera which are present in at least by 50% of overall samples in each groups or in human donors are displayed. W, week; W-6 (week minus 6), murine microbiota before antibiotic treatment. Murine genera are detected only in the mouse stool before antibiotic treatment whereas human genera are detected in the donor stool and present less than 50% in the pre-treatment mouse group. Common genera are found in both the human donor and pre-treatment mouse stools.

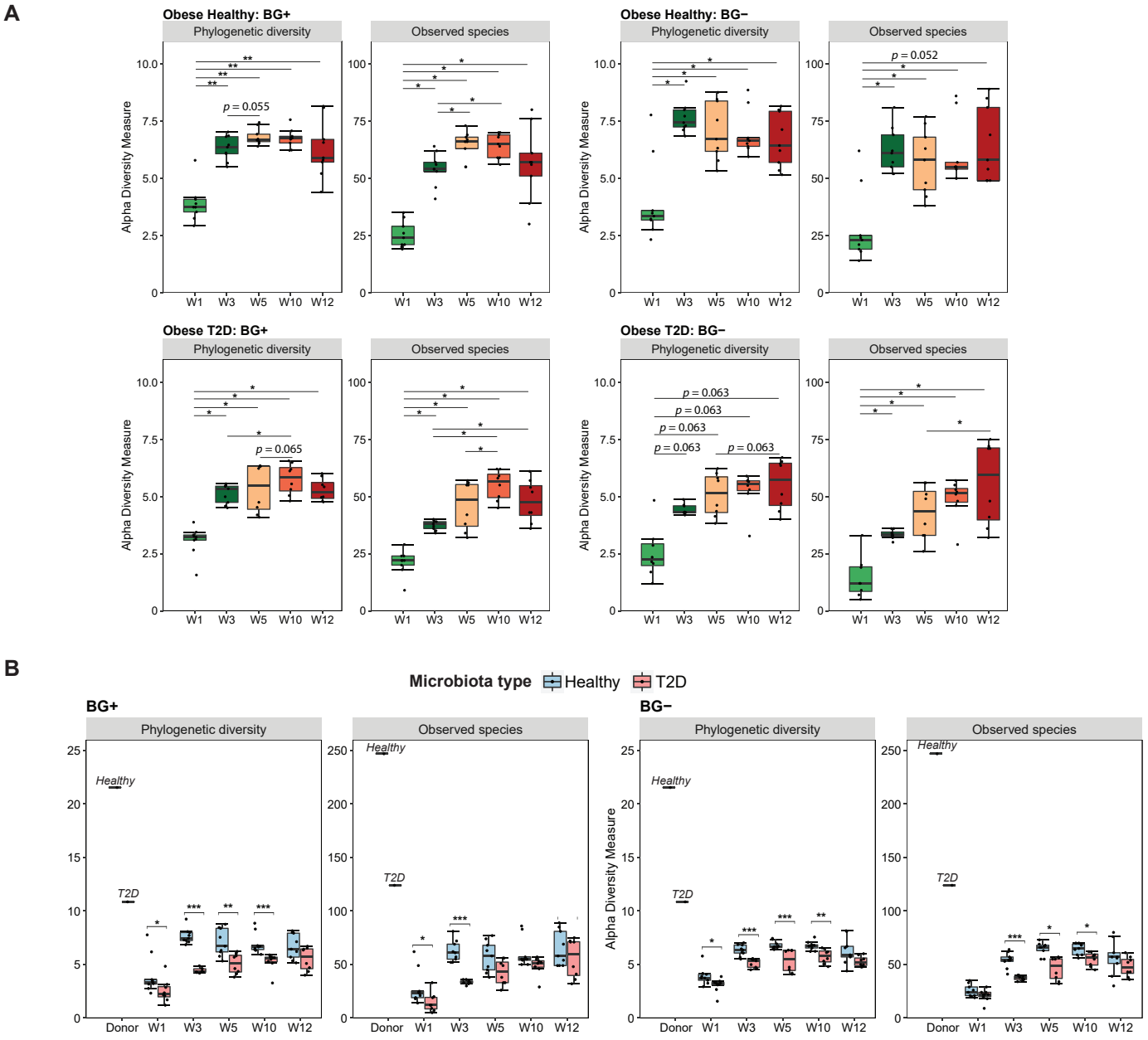

Figure S4. Significant differences in α-diversity in obese healthy and type 2 diabetes inoculated mice with/without β-glucan. (**A**) Significant changes in bacterial α-diversity between time points were calculated using Wilcoxon rank sum test adjusted using Benjamini–Hochberg (BH) correction. (**B**) Alpha diversity comparisons of the gut microbiota between obese type 2 diabetes inoculated mice and obese healthy inoculated mice. Mann-Whitney U tests were performed between two unpaired groups. *$p \leq 0.05$, **$p \leq 0.01$, ***$p \leq 0.001$.

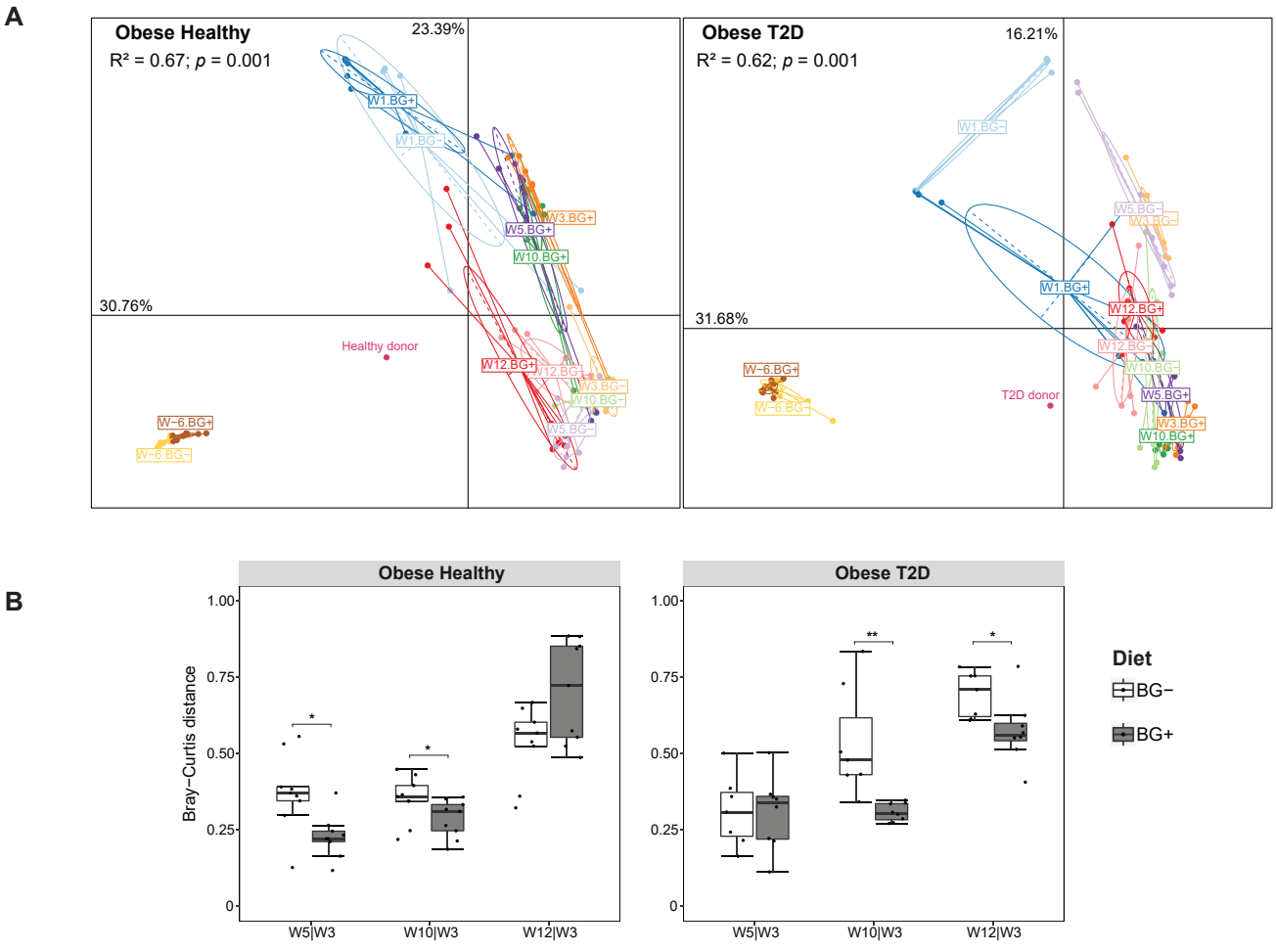

Figure S5. Significant differences in β-diversity between time points in obese healthy and type 2 diabetes inoculated mice with/without β-glucan. (**A**) Principle coordinates analysis plots based on Bray-Curtis dissimilarity visualizing the dissimilarity gut microbiota composition over time. The significant differences among groups were calculated by permutational multivariate analysis of variance (PERMANOVA) tests. (**B**) Boxplots represents the distribution of Bray-Curtis dissimilarity of the faecal microbiota profiles between HFD-diet weeks (W5, W10 and W12) and LFD-diet week (W3) in non β-glucan consumption (BG-) versus β-glucan consumption (BG+). Mann-Whitney U tests were performed between two diet groups. *$p \leq 0.05$, **$p \leq 0.01$.

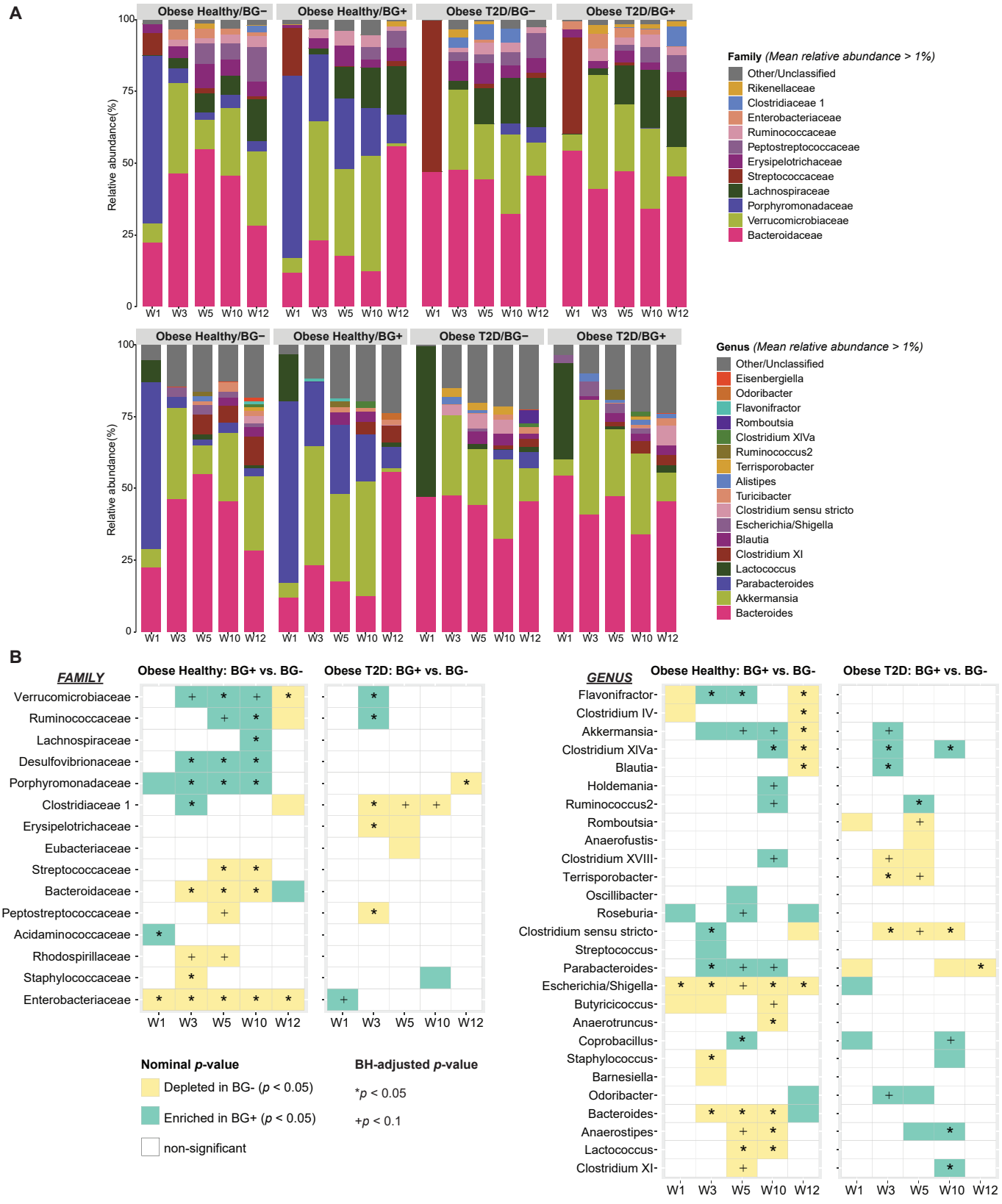

Figure S6. Significantly differentially abundant taxa at family level and genus level in obese type 2 diabetes microbiota inoculated mice or obese healthy inoculated mice associated with β-glucan consumption at each time point. (**A**) Mean relative abundance of the represented microbial taxa. Only taxa having a mean relative abundance of >1% are shown. (**B**) The significant differences in taxa between two diet groups were determined by Mann–Whitney U adjusted using Benjamini–Hochberg correction.

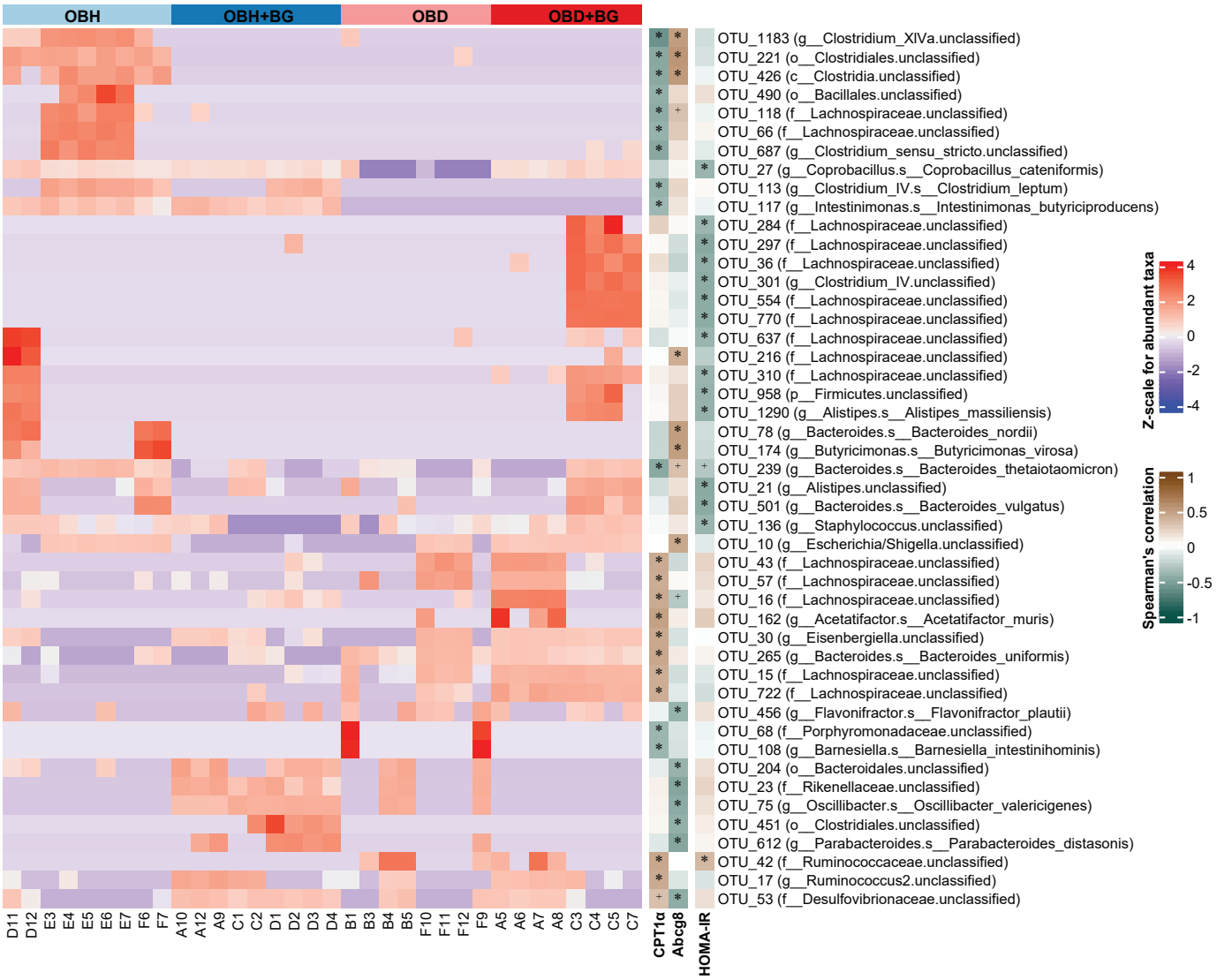

Figure S7. Heatmap showing correlations between the relative abundance of bacterial OTUs at week 10 and the expression of *Cpt1α, Abcg8* genes and HOMA-IR. Bacterial OTUs with Spearman's correlation coefficient value greater than 0.4 are shown. Significance correlations are indicated by * for nominal *p*-values < 0.05 and $^{+}$ for $0.05 \leq p < 0.1$. Abbreviation: o_, order; f_, family; g_, genus; s_, species.

Supplemental Tables.

Table S1. Clinical characteristics of participants, grouped by diabetes status

Characteristics	Obese Healthy (n = 15)	Obese T2D (n = 10)	*P*-value
Age (years)	50.1 ± 9.4	49.4 ± 9.2	0.87†
Weight (kg)	128.7 ± 28.2	140.2 ± 37.4	0.77†
BMI (kg/m^2)	45 ± 6.7	46.5 ± 11.2	0.72†
Fasting glucose (mmol/L)	4.7 ± 0.3	9.1 ± 5.3	0.002†
HbA1c (mmol/mol)	34.6 ± 2.1	59 ± 24.2	0.001†
Gender (#female:male)	7:8	2:8	0.23‖
Artificial sweeteners (# no:yes)	8:7	7:3	0.68‖
Metformin treated (#no:yes)	15:0	2:8	< 0.001‖

Data are expressed as mean ± SD.
P-value was calculated by Kruskal-Wallis test (†) and Fisher's exact test (‖).

Table S2. Clinical characteristics of study participants

Group	Subject code	Gender	Metformin treated	Age (years)	Weight (kg)	BMI (kg/m^2)	Fasting glucose (mmol/L)	HbA1c (mmol/mol)	Diabetes diagnosis	Donor selected for mouse study	Relevant Medication*
Obese Healthy	IM005	Female	No	54	97.2	40.98	5	36	No	No	Elthroxine 75mg OD
	IM008	Female	No	57	118.8	44.71	5	35	No	No	Difene 75 mg OD
	IM028	Female	No	49	97.3	36.2	4.4	36	No	No	Effexor 225mg OD
	IM031	Female	No	59	84.8	30.8	4	31	No	No	Methotrexate 10mg x2 Once a week; Hydroxychloroquine 200mg x2 Daily; Elthroxine 100mg Daily; Folic acid 5mg Once a week; Esomeprazole 20mg Daily; Paroxetine 20mg Daily; Multivitamin A-Z 1 Daily
	IM004	Male	No	45	185.4	55.97	4.8	32	No	No	Fybogel OD
	IM015	Male	No	49	133.6	46.2	4.9	38	No	No	None
	IM017	Male	No	46	132.8	45.2	N/A	37	No	No	Atorvastatin 10mg OD; Nuprin,aspirin 75mg OD; Lecalpin 20mg OD; Pain patch PRN 20mg
	IM024	Male	No	32	149.1	44.1	4.8	34	No	No	Lexapro 10mg OD; Xenacol 120mg TDS; Synex spray PRN; Ventolin PRN
	IM002	Female	No	41	142	53.4	4.6	32	No	No	Ponstan 500mg 1/month
	IM012	Female	No	61	91	36.9	4.6	32	No	No	Arcoxia 90mg OD; Codipar 15 mg BD; Lipitor 10mg OD; Ventolin PRN
	IM014	Female	No	35	112.8	49.5	4.5	35	No	No	Elthroxine 125mg/75mg OD (alternate days); Fybogel OD
	IM010	Male	No	56	135.4	44.7	4.8	35	No	No	Stilnoct 10mg OD; Zispin 30mg OD; Oxycontin 10mg OD; Lexapro 20mg OD; Arcoxia 90mg OD
	IM022	Male	No	55	145.8	48.7	4.8	37	No	No	Micardis plus 80mg OD; Furosemide 40mg OD; Ibuprofen PRN
	IM023	Male	No	48	161.9	50.5	4.5	35	No	No	None
	IM032	Male	No	65	142.2	46.4	4.5	34	No	Healthy donor	Atorvastatin 20mg OD; Bisoprolol 10mg OD; Nuprin 75mg OD; Ramipril 5mg OD; Dilzem 240mg OD; Bendroflumethiazide 2.5mg
Obese T2D/ metformin-	IM003	Male	No	38	209.4	67.6	18.4	90	Yes	T2D donor	None
	IM013	Female	No	50	107	43.98	4.2	31	Yes	No	Eltroxin 100mg OD + 50mg OD; Acerycal 10mg OD; Nebilet 2.5mg OD; Low Centyl K OD; Aspirin 75mg OD; Seretide (inhaler); Spiriva (inhaler); Salamol (inhaler)
Obese T2D/ metformin +	IM001	Male	Yes	44	164.6	51.4	6.9	45	Yes	No	Glucophage 500mg OD; Ramipril 2.5mg OD; Pantoprazole 40mg OD
	IM006	Male	Yes	59	131.6	44.5	5.6	38	Yes	No	Spiriva 2.5mg; Rivaroxaban 20mg OD; Glucophage 500mg BD; Terbinafine 250mg OD; Lyrica 50mg OD; Coversyl 5mg OD; Paracetamol 500mg PRN; Atorvastatin OD; Nebivolol 5mg half tablet OD; Tramadol 50mg BD

IM016	Male	Yes	62	110.4	35.2	5.6	69	Yes	No	Warfarin 12mg OD; Lantus 30 units BD; Victoza 1.24 OD; Glucophage 1000mg BD; Aspirin 75mg OD; Lipitor 10mg OD; Ramipril 2.5mg OD; Bisoprolol 3.75mg
IM021	Male	Yes	46	112.6	34.8	7.9	70	Yes	No	Metformin 1000mg BD; Elthroxine 100mg/75mg (4 days/3days); Movicol
IM029	Male	Yes	55	196.4	63	N/A	43	Yes	No	Calcichew 500mg BD; Atorvastatin 10mg OD; Atenomel 100mg OD; Valsartan 1.25mg OD; Metformin 1000mg BD; Burinex 1mg OD; Elthroxine 100mg OD; Venloflex 150mg BD
IM030	Male	Yes	37	112	37	7.7	49	Yes	No	Glucophage 3xDaily - 1000mg
IM026	Female	Yes	43	119	42.7	7.8	49	Yes	No	Victoza 1.8mg OD; Cerazette OD; Glucophage 1000mg OD; Zirtek 10mg OD; Ventolin inhaler; Seretide inhaler; Cod liver oil capsule OD; Ramipril 2.5mg OD
IM027	Male	Yes	60	138.8	44.8	18.2	106	Yes	No	Glucophage 1g TDS; Simvastatin 20mg OD; Lexapro 10mg OD Aspirin 75mg OD; Elthroxine 25mg OD; Bisoprolol 5mg BD; Pradaxia 10mg BD; Furosemide 40mg OD/ 20mg OD; Hydralazine 25mg TDS; Imdur half tablet OD

*OD: once daily; BD, twice daily, TDS, three times daily

Table S3. Hepatic fatty acid composition Values are expressed as mg fatty acid per g of hepatic tissue (mg/g).

Fatty Acid	OBH		OBH+BG		OBD		OBD+BG		*p-value*
	(*n*=9)		(*n*=9)		(*n*=8)		(*n*=9)		
	Mean	SD	Mean	SD	Mean	SD	Mean	SD	
C16:0 Palmitic	40.42	21.17	59.81	17.49	62.88	9.11	54.81	38.81	0.2746
C16:1n7c Palmitoleic	5.36	3.62	8.58	2.73	8.04	2.19	7.95	6.14	0.4073
C18:0 Stearic	5.75	1.86	6.14	0.99	6.84	0.38	6.22	1.85	0.5388
C18:1n9c Oleic	58.73	36.76	94.86	31.64	97.87	19.87	86.04	67.02	0.2526
C18:2n6c Linoleic	14.65	6.48	19.16	4.14	21.27	1.11	17.73	9.27	0.2073
C18:3n6c Gamma-linolenic	0.37	0.11	0.50	0.10	0.56	0.02	0.47	0.23	0.0807
C18:3:n3 Alpha Linolenic	0.26	0.15	0.32	0.07	0.34	0.03	0.30	0.16	0.5439
C20:4n6 Arachidonic	23.21	2.48	24.34	5.55	21.92	2.36	22.57	3.21	0.5939
C22:5n3c Docosapentaenoic	2.64	0.49	3.11	0.38	3.32	0.42	3.05	0.75	*0.0463*
C22:6n3 Docosahexaenoic	0.28	0.11	0.38	0.10	0.46	0.09	0.31	0.17	*0.027*
n-6:n-3	12.06	1.71	11.58	1.75	10.60	1.47	11.12	2.62	0.3129
Total SFA	46.17	23.53	65.95	18.85	69.72	9.50	61.03	41.78	0.2939
Total MUFA	64.09	46.07	103.44	40.08	105.91	26.16	93.99	84.81	0.2629
Total PUFA	41.40	7.48	47.79	9.92	47.87	2.85	44.44	12.59	0.2298
Total SFA:Total PUFA	1.11515	0.34	1.38	0.21	1.46	0.17	1.37	0.58	0.354
Total Fatty Acid	151.66	76.27	217.18	66.75	223.50	35.57	199.46	138.25	0.2601

Table S4. OBH vs OBD Canonical Pathways Key regulatory pathways that are most differentially modulated ranked either by –log(*p*-value) or z-score representing inhibited or activated expression.

INGENUITY CANONICAL PATHWAYS	-LOG(*P*-VALUE)	EXPRESSION	Z-SCORE	MOLECULES
MITOCHONDRIAL DYSFUNCTION	6.31E+01			ACO1,ACO2,AIFM1,ATP5F1A,ATP5F1B,ATP5F1C,ATP5F1D,ATP5F1E,ATP5MC2,ATP5ME, ATP5MF,ATP5MG,ATP5PB,ATP5PD,ATP5PF,ATP5PO,CASP8,CAT,COX15,COX4I1,COX5A, COX5B,COX6A1,COX6B1,COX6C,COX7A2,COX7C,CPT1A,CYB5A,CYB5R3,CYC1,CYCS, FIS1,GPD2,GPX4,GSR,HSD17B10,HTRA2,MAOA,MAOB,MAP2K4,MT-ATP6,MT-CO1,MT-CO2,MT-CO3,MT-ND1,MT-ND3,MT-ND4,MT-ND5,NDUFA10,NDUFA11,NDUFA12, NDUFA13,NDUFA2,NDUFA3,NDUFA4,NDUFA5,NDUFA6,NDUFA7,NDUFA8,NDUFA9, NDUFAB1,NDUFAF2,NDUFB1,NDUFB10,NDUFB11,NDUFB2,NDUFB3,NDUFB4,NDUFB5, NDUFB6,NDUFB7,NDUFB8,NDUFB9,NDUFS1,NDUFS2,NDUFS3,NDUFS4,NDUFS5,NDUFS6,NDUFS7,NDUFS8,NDUFV1,NDUFV2,NDUFV3,OGDH,PARK7,PDHA1,PRDX3,PRDX5,SDHA,SDHB,SDHC,SDHD,SOD2,SURF1,TXN2,TXNRD2,UQCR10,UQCRB,UQCRC1,UQCRC2, UQCRFS1,UQCRH,UQCRQ,VDAC1,VDAC2,VDAC3,XDH
EIF2 SIGNALING	5.85E+01			ACTA2,ACTB,ACTC1,AKT2,EIF1,EIF2A,EIF2B1,EIF2B2,EIF2B5,EIF2S1,EIF2S2,EIF3A, EIF3B,EIF3C,EIF3D,EIF3E,EIF3F,EIF3G,EIF3H,EIF3I,EIF3K,EIF3L,EIF3M,EIF4A1,EIF4A2, EIF4E,EIF4G1,EIF4G2,EIF5,EIF5B,FAU,GRB2,HNRNPA1,HRAS,HSPA5,MAP2K1,MAP2K2, MAPK1,MAPK3,PABPC1,PPP1CA,PPP1CB,PPP1CC,PTBP1,RALB,RAP1B,RPL10,RPL10A, RPL12,RPL13,RPL13A,RPL14,RPL15,RPL17,RPL18,RPL18A,RPL19,RPL21,RPL22,RPL22L1, RPL23,RPL23A,RPL24,RPL26,RPL27,RPL27A,RPL28,RPL29,RPL3,RPL30,RPL31,RPL32, RPL34,RPL35,RPL35A,RPL36,RPL37A,RPL38,RPL39,RPL4,RPL5,RPL6,RPL7,RPL7A,RPL8, RPL9,RPLP0,RPLP2,RPS10,RPS11,RPS13,RPS14,RPS15,RPS15A,RPS16,RPS17,RPS18,RPS19, RPS2,RPS20,RPS21,RPS23,RPS24,RPS25,RPS26,RPS27,RPS27A,RPS27L,RPS28,RPS29,RPS3, RPS3A,RPS4X,RPS5,RPS6,RPS7,RPS8,RPS9,RPSA,RRAS,WARS1
OXIDATIVE PHOSPHORYLATION	5.38E+01			ATP5F1A,ATP5F1B,ATP5F1C,ATP5F1D,ATP5F1E,ATP5MC2,ATP5ME,ATP5MF,ATP5MG,ATP5PB,ATP5PD,ATP5PF,ATP5PO,COX15,COX4I1,COX5A,COX5B,COX6A1,COX6B1,COX6C,COX7A2,COX7C,CYB5A,CYC1,CYCS,MT-ATP6,MT-CO1,MT-CO2,MT-CO3,MT-ND1,MT-ND3,MT-ND4,MT-ND5,NDUFA10,NDUFA11,NDUFA12,NDUFA13, NDUFA2,NDUFA3,NDUFA4,NDUFA5,NDUFA6,NDUFA7,NDUFA8,NDUFA9,NDUFAB1,NDUFB1,NDUFB10,NDUFB11,NDUFB2,NDUFB3,NDUFB4,NDUFB5,NDUFB6,NDUFB7,NDUFB8,NDUFB9,NDUFS1,NDUFS2,NDUFS3,NDUFS4,NDUFS5,NDUFS6,NDUFS7,NDUFS8,NDUFV1,NDUFV2,NDUFV3,SDHA,SDHB, SDHC,SDHD,SURF1,UQCR10,UQCRB,UQCRC1, UQCRC2,UQCRFS1,UQCRH,UQCRQ
SIRTUIN SIGNALING PATHWAY	3.98E+01			ACADL,ACLY,ACSS2,APEX1,ATG3,ATG7,ATP5F1A,ATP5F1B,ATP5F1C,ATP5F1D,ATP5F1E,ATP5PB,ATP5PF,BPGM,CPS1,CPT1A,CYC1,GLUD1,GOT2,H1-0,H1-2,H1-3,H1-4,H1-5,H3-3A/H3-3B,HMGCS2,IDH2,LDHA,LDHD,MAPK1,MAPK3,MLYCD,MT-ATP6,MT-ND1,MT-ND3,MT-ND4,MT-ND5,NAMPT,NDRG1,NDUFA10,NDUFA11,NDUFA12,NDUFA13, NDUFA2,NDUFA3,NDUFA4,NDUFA5,NDUFA6,NDUFA7,NDUFA8,NDUFA9,NDUFAB1, NDUFAF2,NDUFB1,NDUFB10,NDUFB11,NDUFB2,NDUFB3,NDUFB4,NDUFB5,NDUFB6, NDUFB7,NDUFB8,NDUFB9,NDUFS1,NDUFS2,NDUFS3,NDUFS4,NDUFS5,NDUFS6, NDUFS7,NDUFS8,NDUFV1,NDUFV2,NDUFV3,NEDD4,OTC,PCK1,PDHA1,PDK1,PGAM1, PGK1,PPID,PPIF,PRKAA2,SDHA,SDHB,SDHC,SDHD,SF3A1,SIRT2,SIRT3,SIRT5,SLC25A5, SOD1,SOD2,SOD3,STAT3,TIMM13,TIMM23,TIMM44,TIMM50,TOMM22,TOMM40, TOMM70,TRIM28,TSPO,TUBA1A,TUBA1B,TUBA1C,TUBA4A,UQCRC2,UQCRFS1,VDAC1, VDAC2,VDAC3,XRCC5
REGULATION OF EIF4 AND P70S6K SIGNALING	3.45E+01			AKT2,EIF1,EIF2A,EIF2B1,EIF2B2,EIF2B5,EIF2S1,EIF2S2,EIF3A,EIF3B,EIF3C,EIF3D,EIF3E, EIF3F,EIF3G,EIF3H,EIF3I,EIF3K,EIF3L,EIF3M,EIF4A1,EIF4A2,EIF4E,EIF4EBP2,EIF4G1,EIF4G2,FAU,GRB2,HRAS,ITGA5,ITGB1,MAP2K1,MAP2K2,MAPK1,MAPK14,MAPK3,PABPC1, PPP2CA,PPP2R1A,PPP2R2A,PPP2R5A,PPP2R5D,PPP2R5E,PTPA,RALB,RAP1B,RPS10,

				RPS11,RPS13,RPS14,RPS15,RPS15A,RPS16,RPS17,RPS18,RPS19,RPS2,RPS20,RPS21,RPS23, RPS24,RPS25,RPS26,RPS27,RPS27A,RPS27L,RPS28,RPS29,RPS3,RPS3A,RPS4X,RPS5,RPS6, RPS7,RPS8,RPS9,RPSA,RRAS
TRNA CHARGING	1.06E+01	Inhibited	-3.7097	AARS1,CARS1,DARS1,EPRS1,FARSA,FARSB,GARS1,HARS1,IARS1,IARS2,KARS1,LARS1, MARS1,NARS1,RARS1,SARS1,TARS1,TARS2,VARS,WARS1,YARS1
EIF2 SIGNALING	5.85E+01	Inhibited	-3.1497	ACTA2,ACTB,ACTC1,AKT2,EIF1,EIF2A,EIF2B1,EIF2B2,EIF2B5,EIF2S1,EIF2S2,EIF3A, EIF3B,EIF3C,EIF3D,EIF3E,EIF3F,EIF3G,EIF3H,EIF3I,EIF3K,EIF3L,EIF3M,EIF4A1,EIF4A2, EIF4E,EIF4G1,EIF4G2,EIF5,EIF5B,FAU,GRB2,HNRNPA1,HRAS,HSPA5,MAP2K1,MAP2K2, MAPK1,MAPK3,PABPC1,PPP1CA,PPP1CB,PPP1CC,PTBP1,RALB,RAP1B,RPL10,RPL10A, RPL12,RPL13,RPL13A,RPL14,RPL15,RPL17,RPL18,RPL18A,RPL19,RPL21,RPL22,RPL22L1, RPL23,RPL23A,RPL24,RPL26,RPL27,RPL27A,RPL28,RPL29,RPL3,RPL30,RPL31,RPL32, RPL34,RPL35,RPL35A,RPL36,RPL37A,RPL38,RPL39,RPL4,RPL5,RPL6,RPL7,RPL7A,RPL8, RPL9,RPLP0,RPLP2,RPS10,RPS11,RPS13,RPS14,RPS15,RPS15A,RPS16,RPS17,RPS18,RPS19, RPS2,RPS20,RPS21,RPS23,RPS24,RPS25,RPS26,RPS27,RPS27A,RPS27L,RPS28,RPS29,RPS3, RPS3A,RPS4X,RPS5,RPS6,RPS7,RPS8,RPS9,RPSA,RRAS,WARS1
SUPERPATHWAY OF CITRULLINE METABOLISM	5.38E+00	Inhibited	-3	ARG1,ASL,ASS1,CPS1,GLS2,LOC102724788/PRODH,OAT,OTC,PRODH2
UNFOLDED PROTEIN RESPONSE	7.79E+00	Inhibited	-2.82843	AMFR,CALR,CANX,DNAJA2,DNAJC3,EIF2A,ERO1B,HSP90B1,HSPA1A/HSPA1B,HSPA1L, HSPA4,HSPA5,HSPA8,HSPA9,HSPH1,OS9,P4HB,PDIA2,PDIA6,SEL1L,UBXN4,VCP
CITRULLINE BIOSYNTHESIS	4.08E+00	Inhibited	-2.44949	ARG1,GLS2,LOC102724788/PRODH,OAT,OTC,PRODH2
GALACTOSE DEGRADATION I (LELOIR PATHWAY)	4.90E+00	Activated	2.236068	GALE,GALK1,GALK2,GALM,GALT
RHOGDI SIGNALING	4.32E+00	Activated	2.26301	ACTA2,ACTB,ACTC1,ACTG1,ACTR2,ACTR3,ARHGDIA,ARHGDIB,ARPC1A,ARPC1B, ARPC2,ARPC3,ARPC4,ARPC5,CDC42,CDH2,CFL1,CFL2,EZR,GNAI2,GNAS,GNB2,GNG12, GNG5,ITGA5,ITGB1,MSN,MYL12B,MYL6,PAK2,PI4KA,PIP4K2C,RAC1,RDX,RHOA, RHOT1,WASF2
SPINK1 PANCREATIC CANCER PATHWAY	1.69E+00	Activated	2.309401	CELA1,CELA2A,CELA3B,CPA1,CPB1,CPQ,CTRL,CTSA,CTSB,KLK1,KLKB1,PRSS2
NRF2-MEDIATED OXIDATIVE STRESS RESPONSE	2.30E+01	Activated	2.333333	ABCC2,ACTA2,ACTB,ACTC1,ACTG1,AKR1A1,AKR7A2,AOX1,CAT,CBR1,CCT7,CLPP, CUL3,DNAJA1,DNAJA2,DNAJA3,DNAJB1,DNAJB11,DNAJB4,DNAJC11,DNAJC13,DNAJC3 DNAJC7,EPHX1,ERP29,FMO1,FTH1,GCLC,GCLM,GSR,GSTA2,GSTA3,GSTA4,GSTK1, GSTM1,GSTM2,GSTM3,GSTM4,GSTM5,GSTO1,GSTP1,GSTT1,GSTT2/GSTT2B,GSTZ1, HACD3,HRAS,HSPB8,MAP2K1,MAP2K2,MAP2K3,MAP2K4,MAPK1,MAPK14,MAPK3, MGST1,NQO2,PPIB,PRDX1,RALB,RAP1B,RRAS,SCARB1,SOD1,SOD2,SOD3,SQSTM1, STIP1,TXN, TXNRD1,UBE2K,USP14,VCP
GLUCONEOGENESIS I	8.31E+00	Activated	2.840188	ALDOA,ALDOB,ALDOC,BPGM,ENO1,ENO3,FBP1,GAPDH,GPI,MDH1,MDH2,ME1,PGAM1, PGK1,PGK2

Table S5. OBH vs OBD Upstream Regulators

UPSTREAM REGULATOR	MOLECULE TYPE	PREDICTED ACTIVATION STATE	ACTIVATION Z-SCORE	MECHANISTIC NETWORK
MYCN	transcription regulator	Inhibited	-4.653	FOXO1,FOXO3,MYC,MYCN,PPARG,RNA polymerase II,SP1,TP53
MYC	transcription regulator	Inhibited	-4.381	AHR,ARNT,ESR1,ESR2,FOS,FOXO1,FOXO3,HIF1A,JUN,MAX,MYC,MYCN,NR3C1,PPARG,SP1,TP53,VHL,beta-estradiol
GCG (GLUCAGON)	Protein coding	Inhibited	-3.893	
ACOX1	enzyme	Inhibited	-3.764	ACOX1,CEBPA,Esrra,FOXO1,FOXO3,MYC,PPARA,PPARD,PPARG,RXRA,SP1,SREBF1,TP53,fatty acid
CLPP	peptidase	Inhibited	-3.677	
PPARG	ligand-dependent nuclear receptor	Activated	2.882	ATF4,CEBPA,Esrra,FOXO1,JUN,MLXIPL,MYC,NR1H4,NR1I3,PPARA,PPARG,PPARGC1A,RXRA,SIRT1,SP1,SREBF1,THRB,TP53,rosiglitazone, troglitazone
FOXA2	transcription regulator	Activated	2.884	CEBPB,FOXA2,FOXA3,Ins1,ONECUT1,PPARA,PPARG,PPARGC1A,RXRA,SREBF1
PCGEM1	other	Activated	3.134	HIF1A,JUN,MAX,MYC,PCGEM1,SP1,TP53
ACSS2	enzyme	Activated	3.148	ACSS2,FOXO1,PPARA,RXRA,SIRT1,SREBF1,ethanol
PNPLA2	enzyme	Activated	3.874	CEBPA,CTNNB1,D-glucose, Esrra, FOXO1, HIF1A, JUN,LEP,MLXIPL,MYC,PDX1,PNPLA2,PPARA,PPARD,PPARG,PPARGC1A,RXRA,SP1,SP3,SREBF1,palmitic acid
PPARA	ligand-dependent nuclear receptor	Activated	5.631	CEBPA,CEBPB,FOXO1,JUN,NR1H4,NR1I3,PPARA,PPARD,PPARG,PPARGC1A,RXRA,SREBF1,THRB,bezafibrate,fenofibrate,pirinixic acid

Table S6. OBD vs OBD+β-glucan Canonical Pathways Key regulatory pathways that are most differentially modulated ranked either by –log(*p*-value) or z-score representing inhibited or activated expression.

INGENUITY CANONICAL PATHWAYS	-LOG(*P*-VALUE)	EXPRESSION	Z-SCORE	MOLECULES
EIF2 SIGNALING	9.65			EIF3E,EIF4G1,PTBP1,RPL18,RPL28,RPL5,RPL6,RPS10, RPS15A,RPS20,RPS23,RPS27A,RPS4X
REGULATION OF EIF4 AND P70S6K SIGNALING	6.78			EIF3E,EIF4G1,PPP2CA,RPS10,RPS15A,RPS20,RPS23, RPS27A,RPS4X
MTOR SIGNALING	5.72			EIF3E,EIF4G1,PPP2CA,RPS10,RPS15A,RPS20,RPS23, RPS27A,RPS4X
MITOCHONDRIAL DYSFUNCTION	4.43			AIFM1,MT-ND4,NDUFB11,NDUFB9,NDUFS3,OGDH,XDH
TRNA CHARGING	4.26			EPRS1,FARSA,RARS1,SARS1
SIRTUIN SIGNALING PATHWAY	1.7	Inhibited	-1.34164	MT-ND4,NDUFB11,NDUFB9,NDUFS3,XRCC5
OXIDATIVE PHOSPHORYLATION	2.56	Activated	1	MT-ND4,NDUFB11,NDUFB9,NDUFS3
TRNA CHARGING	4.26	Activated	2	EPRS1,FARSA,RARS1,SARS1
EIF2 SIGNALING	9.65	Activated	2	EIF3E,EIF4G1,PTBP1,RPL18,RPL28,RPL5,RPL6,RPS10, RPS15A,RPS20,RPS23,RPS27A,RPS4X

Table S7. OBD vs OBD+β-glucan Upstream Regulators

UPSTREAM REGULATOR	MOLECULE TYPE	PREDICTED ACTIVATION STATE	ACTIVATION Z-SCORE
RICTOR	other	Inhibited	-2.121
INS1	other	Inhibited	-2
BDNF	growth factor	Inhibited	-1.982
NFE2L2	transcription regulator	Activated	1.697
XBP1	transcription regulator	Activated	1.982
SYVN1	transporter	Activated	2
MYC	transcription regulator	Activated	2.175
MYCN	transcription regulator	Activated	2.538

Supplemental Text.

Methods

Genomic DNA extraction and microbiota profiling based on 16S rRNA gene sequencing

Total DNA was extracted from human faecal samples and murine faecal pellets using the QIamp Fast DNA Stool (Qiagen, Manchester, U.K.) kit. Briefly, the samples were weighted and placed into sterile tubes containing 0.1, 0.5, and 1.0 mm zirconia/glass beads (Thistle Scientific, U.K.) and homogenized in InhibitEX buffer using a Mini-Beadbeader (Biospec Products, USA). Specifically, samples were homogenized in two intervals (1 min and 40 s) with an intermediate step when the samples were placed on ice for 1 min. The samples were then placed in a 95 °C heat-block for 5 min. The subsequent steps of the DNA extraction were carried out as described in the Qiagen protocol. The obtained genomic DNA was used as a template in library preparation for 16S rRNA gene amplicon sequencing.

The V3-V4 variable region of the 16S rRNA gene was amplified using the universal 16S rRNA gene primer pair S-D-Bact-0341-b-S-17 (5'-CCTACGGGNGGCWGCAG-3')/S-D-Bact-0785-a-A-21 (5'-GACTACHVGGGTATCTAATCC-3') [1]. Amplification was performed in 30 μL containing 2 μL of template DNA (final concentration 15 ng/μL), 15 μL of 2x Phusion High-Fidelity PCR Master Mix (ThermoFisher Scientific, Waltham, MA, USA), 1.2 μL of each 16S primer (final concentration 0.2 μM) and 10.6 μL of nuclease-free H_2O. The cycling conditions were as follows: initial denaturation at 98 °C for 30 s; 25 cycles at 98 °C for 10 s, at 55 °C for 15 s and at 72 °C for 20 s; final extension at 72 °C for 5 min, followed by a hold at 4 °C. The PCR products were purified using the Agencourt AMPure XP-PCR Purification system (Beckman Coutler, Inc., California, USA), and the subsequent library preparation steps were performed according to the Illumina MiSeq system protocol. Dual-index barcodes were attached to the amplicon (Nextera XT V.2 Index Kits sets A and D, Illumina) and then purified as before. The indexed amplicons were quantified using the Qubit dsDNA HS Assay Kit (Thermo Fischer Scientific, MA, USA). Purified amplicons were pooled in equal volumes. Sequencing (2 x 250 bp) of the pooled library was performed using the Illumina MiSeq instrument (Illumina, Inc., San Diego, CA, USA) in the Eurofins GATC Biotech GmbH (Constance, Germany).

Library preparation and shotgun metagenomic sequencing

Shotgun libraries were prepared using the Nextera XT DNA Library Prep Kit (Illumina) following the manufacturer's instructions. First, total genomic DNA was quantified using Qubit™ dsDNA HS Assay Kit (Thermo Fisher). One ng genomic DNA of each sample was fragmented by adding 5 µL of Amplicon Tagment Mix with 10 µL of Tagment DNA Buffer. The tagmented DNA were amplified by PCR with 5 µL of each Illumina Nextera index adapters (i5 and i7) and 15 µL of Nextera PCR Master Mix (Nextera XT Index Kit v2 Set B, Illumina). The cycling conditions were as follows: initial denaturation at 95 °C for 30 s; 12 cycles at 95 °C for 30 s, at 55 °C for 30 s and at 72 °C for 30 s; final extension at 72 °C for 5 min, followed by a hold at 10 °C. The PCR products were purified using the Agencourt AMPure XP-PCR Purification system (Beckman Coutler, Inc., California, USA). The shotgun libraries were sequenced using Illumina NextSeq® 500/550 High Output v2 (300 cycles) at the National Irish Sequencing Centre (Teagasc Food Research Centre, Ireland) to generate 150 bp paired-end read libraries according to the manufacturer's instructions.

Bioinformatic analysis of 16S amplicon sequencing data

We applied a similar 16S rRNA gene amplicon pipeline as previously described [2]. The Illumina MiSeq paired-end sequencing reads of V3-V4 16S rRNA regions were first were merged using Fast Length Adjustment of Short Reads (FLASH) v.1.2.8 [3] and trimmed the forward primers using cutadapt v1.8.3 [4]. The reads were filtered with a minimum quality score of 19 using split_libraries_fastq.py and then removed the reversed primers using truncate_reverse_primer.py from QIIME v1.9.1 [5]. The quality-filtered sequences were dereplicated, filtered by length of 373–473nt, removed singleton and were then clustered into Operational Taxonomic Units (OTUs) at a threshold similarity of 97% with the USEARCH v6.1 [6]. The chimeric sequences were discarded using UCHIME against the GOLD reference database [7] and all post-QIIME quality-filtered reads were mapped back to the representative OTU sequences to generate the OTU table using the -usearch_global option from USEARCH. To ensure an even sampling depth, the OTU table was rarefied using QIIME with single_rarefaction.py at a depth of 14,335 reads per sample as the lowest read count in the dataset and used for calculating α- and β- diversity of the gut microbial community with alpha_diversity.py and beta_diversity.py scripts. Taxonomic assignment for each representative OTU sequences were performed using mothur v1.36.1 against the RDP database version 11.5 for genus classification and SPINGO v1.3 against the species reference database

(RDP version 11.2) for species classification [8-10]. For both classifications, sequences with a confidence score below 80% were considered as unclassified.

Hepatic Proteomic Analysis

Protein isolation: Protein was isolated with the addition of trichloroacetic acid (20%). After centrifugation at 14,000rpm for 10 mins and aspiration, cell pellets were twice washed in ice-cold acetone with centrifugation repeated. Protein pellets were resuspended in 8M Urea. Protein concentration was determined using the Bradford Assay.

In-solution digestion: Cysteine residues were reduced using dithiothreitol followed by alkylation with iodoacetamide. Dithiothreitol, iodoacetamide and urea concentrations were diluted using 50mM NH4HCO3 before trypsin singles TM proteomic grade (Sigma) was added, ensuring a urea concentration of less than 2M. Digestion was carried out overnight at 37°C. After drying in vacuum centrifuge, peptides were acidified by acetic acid (AA), desalted with c18 STAGE tips [11], and resuspended in 2.5% acetonitrile (ACN), 0.5% AA.

Mass Spectrometry: Peptide fractions were analyzed on a quadrupole Orbitrap (Q-Exactive, Thermo Scientific) mass spectrometer equipped with a reversed-phase NanoLC UltiMate 3000 HPLC system (Dionex LC Packings, now Thermo Scientific). Peptide samples were loaded onto C18 reversed phase columns (10 cm length, 75 µm inner diameter) and eluted with a linear gradient from 1 to 27% buffer B containing 0.5% AA 97% ACN in 118 min at a flow rate of 250 nL/min. The injection volume was 5 µL. The mass spectrometer was operated in data dependent mode, automatically switching between MS and MS2 acquisition. Survey full scan MS spectra (m/z 300 – 1200) were acquired in the Orbitrap with a resolution of 70,000. MS2 spectra had a resolution of 17,500. The twelve most intense ions were sequentially isolated and fragmented by higher-energy C-trap dissociation.

Protein identification: Raw data from the Orbitrap Q-Exactive was processed using MaxQuant version 1.6.3.4 [12], incorporating the Andromeda search engine [13]. To identify peptides and proteins, MS/MS spectra were matched to the Uniprot *mus mus musculus* database (2018_09) containing 53,780 entries. All searches were performed with tryptic specificity allowing two missed cleavages. The database searches were performed with carbamidomethyl (C) as fixed modification and acetylation (protein N terminus) and oxidation (M) as variable modifications. Mass spectra were searched using the default setting of MaxQuant namely a false discovery rate of 1% on the peptide and protein level. For the generation of label free

quantitative (LFQ) ion intensities for protein profiles, signals of corresponding peptides in different nano-HPLC MS/MS runs were matched by MaxQuant in a maximum time window of 1 min [14].

Proteomic data analysis: The Perseus computational platform (version 1.6.2.3) was used to process MaxQuant results [15]. Data was log transformed. *T*-test comparisons (at *p*-value ≤0.05) were carried out between liver proteomes specifying that a protein needed to be observed in six samples of samples in at least one group. For visualization of data using heat maps, missing values were imputed with values from a normal distribution and the dataset was normalized by z-score. Pathway enrichment analysis was performed using the ClueGo (v2.5.2) [16] and Cluepedia (v1.5.2) [17] plugins in Cytoscape (v3.6.1) [18] with the mus musculus (10090) marker set. The Gene ontology (GO) biological process and reactome pathway databases, consisting of 21,259 and 9,292 genes, were used [19]. GO tree levels (min = 3; max = 8) and GO term restriction (min#genes = 3, min% = 1%) were set and terms were grouped using a Kappa Score Threshold of 0.4. The classification was performed by the right-sided enrichment hypergeometric statistic test, and its probability value was corrected by the Bonferroni method (Adjusted % Term *p*-value ≤0.05) [16].

Results

β-glucan responsive taxa differ between obese type 2 diabetes inoculated mice and obese healthy inoculated mice at family and genus level

Analysis of differentially abundant taxa linked to β-glucan supplementation identified 15 microbial families among which members of the *Verrucomicrobiaceae* and *Ruminococcaceae* families (representing 23.1% of total abundance on average) were negatively associated, and *Peptostreptococcaceae* (occupying 3.4% of total abundance on average) was negatively associated in both obese healthy and type 2 diabetes groups (**Figure S6**). Five significantly differential families detected at week 3 were lost when the diet was switched to HFD except *Clostridiaceae* 1 and *Erysipelotrichaceae* in the obese type 2 diabetes-humanized group. Increased relative abundance of *Verrucomicrobiaceae, Ruminococcaceae, Desulfovibrionaceae, Porphyromonadaceae* and a decrease in *Streptococcaceae, Bacteroidaceae, Rhodospirillaceae, Enterobacteriaceae* were consistently associated with β-glucan consumption from week 3 to week 10. The only exception among the *Enterobacteriaceae* was the genus *Escherichia/Shigella* which was present at all time points in the obese healthy-humanized group (**Figure S6B**). At the genus level, *Parabacteroides* was

the most predominant taxon in the obese healthy inoculated mice, accounting for more than 60% in total abundance, while *Lactococcus* and *Bacteroides* were present in higher proportions (of more than 90% relative abundance in the obese type 2 diabetes) inoculated mice at week 1. These relative abundances decreased in the subsequent weeks, but *Bacteroides* was one of the most abundant genera in both obese healthy and type 2 diabetes-humanized groups at week 1 and remained abundant over time in non-β-glucan diet and obese type 2 diabetes groups, whereas they were less abundant with an average of less than 25% total abundance until week 10 in obese healthy inoculated mice receiving β-glucan (**Figure S6A**). These differences of *Bacteroides* in healthy obese group upon β-glucan supplementation were statistically significant (Mann-Whitney U test, BH-adjusted $p \leq 0.05$, **Figure S6B**). Moreover, 27 genera were associated with β-glucan consumption of which 9 were genera in the obese healthy humanized group and 8 genera in obese type 2 diabetes group which were consistently more or less abundant in mice receiving β-glucan compared to those without β-glucan for at least two time points. *Flavonifractor, Akkermansia, Roseburia, Parabacteroides* in obese healthy group and *Clostridium XlVa, Odoribacter, Anaerostipes* in obese type 2 diabetes group were found in significantly higher proportions in the supplementation with β-glucan.

References

[1] Klindworth, A., Pruesse, E., Schweer, T., Peplies, J., Quast, C., Horn, M., Glockner, F. O., Evaluation of general 16S ribosomal RNA gene PCR primers for classical and next-generation sequencing-based diversity studies. *Nucleic Acids Res* 2013, *41*, e1.

[2] Tran, T. T. T., Cousin, F. J., Lynch, D. B., Menon, R., Brulc, J., Brown, J. R. M., O'Herlihy, E., Butto, L. F., Power, K., Jeffery, I. B., O'Connor, E. M., O'Toole, P. W., Prebiotic supplementation in frail older people affects specific gut microbiota taxa but not global diversity. *Microbiome* 2019, *7*, 39.

[3] Magoc, T., Salzberg, S. L., FLASH: fast length adjustment of short reads to improve genome assemblies. *Bioinformatics* 2011, *27*, 2957-2963.

[4] Martin, M., Cutadapt removes adapter sequences from high-throughput sequencing reads. *EMBnet J* 2011, *17*, 10-12.

[5] Caporaso, J. G., Kuczynski, J., Stombaugh, J., Bittinger, K., Bushman, F. D., Costello, E. K., Fierer, N., Pena, A. G., Goodrich, J. K., Gordon, J. I., Huttley, G. A., Kelley, S. T., Knights, D., Koenig, J. E., Ley, R. E., Lozupone, C. A., McDonald, D., Muegge, B. D., Pirrung, M., Reeder, J., Sevinsky, J. R., Turnbaugh, P. J., Walters, W. A., Widmann, J., Yatsunenko, T., Zaneveld, J., Knight, R., QIIME allows analysis of high-throughput community sequencing data. *Nat Methods* 2010, *7*, 335-336.

[6] Edgar, R. C., Search and clustering orders of magnitude faster than BLAST. *Bioinformatics* 2010, *26*, 2460-2461.

[7] Haas, B. J., Gevers, D., Earl, A. M., Feldgarden, M., Ward, D. V., Giannoukos, G., Ciulla, D., Tabbaa, D., Highlander, S. K., Sodergren, E., Methe, B., DeSantis, T. Z., Human Microbiome, C., Petrosino, J. F., Knight, R., Birren, B. W., Chimeric 16S rRNA sequence formation and detection in Sanger and 454-pyrosequenced PCR amplicons. *Genome Res* 2011, *21*, 494-504.

[8] Allard, G., Ryan, F. J., Jeffery, I. B., Claesson, M. J., SPINGO: a rapid species-classifier for microbial amplicon sequences. *BMC Bioinformatics* 2015, *16*, 324.

[9] Cole, J. R., Wang, Q., Fish, J. A., Chai, B., McGarrell, D. M., Sun, Y., Brown, C. T., Porras-Alfaro, A., Kuske, C. R., Tiedje, J. M., Ribosomal Database Project: data and tools for high throughput rRNA analysis. *Nucleic Acids Res* 2014, *42*, D633-642.

[10] Schloss, P. D., Westcott, S. L., Ryabin, T., Hall, J. R., Hartmann, M., Hollister, E. B., Lesniewski, R. A., Oakley, B. B., Parks, D. H., Robinson, C. J., Sahl, J. W., Stres, B., Thallinger, G. G., Van Horn, D. J., Weber, C. F., Introducing mothur: open-source, platform-independent, community-supported software for describing and comparing microbial communities. *Appl Environ Microbiol* 2009, *75*, 7537-7541.

[11] Rappsilber, J., Mann, M., Ishihama, Y., Protocol for micro-purification, enrichment, pre-fractionation and storage of peptides for proteomics using StageTips. *Nat Protoc* 2007, *2*, 1896-1906.

[12] Cox, J., Mann, M., MaxQuant enables high peptide identification rates, individualized p.p.b.-range mass accuracies and proteome-wide protein quantification. *Nat Biotechnol* 2008, *26*, 1367-1372.

[13] Cox, J., Neuhauser, N., Michalski, A., Scheltema, R. A., Olsen, J. V., Mann, M., Andromeda: a peptide search engine integrated into the MaxQuant environment. *J Proteome Res* 2011, *10*, 1794-1805.

[14] Cox, J., Hein, M. Y., Luber, C. A., Paron, I., Nagaraj, N., Mann, M., Accurate proteome-wide label-free quantification by delayed normalization and maximal peptide ratio extraction, termed MaxLFQ. *Mol Cell Proteomics* 2014, *13*, 2513-2526.

[15] Tyanova, S., Temu, T., Sinitcyn, P., Carlson, A., Hein, M. Y., Geiger, T., Mann, M., Cox, J., The Perseus computational platform for comprehensive analysis of (prote)omics data. *Nat Methods* 2016, *13*, 731-740.

[16] Bindea, G., Mlecnik, B., Hackl, H., Charoentong, P., Tosolini, M., Kirilovsky, A., Fridman, W. H., Pagès, F., Trajanoski, Z., Galon, J., ClueGO: a Cytoscape plug-in to decipher functionally grouped gene ontology and pathway annotation networks. *Bioinformatics* 2009, *25*, 1091-1093.

[17] Bindea, G., Galon, J., Mlecnik, B., CluePedia Cytoscape plugin: pathway insights using integrated experimental and in silico data. *Bioinformatics* 2013, *29*, 661-663.

[18] Shannon, P., Markiel, A., Ozier, O., Baliga, N. S., Wang, J. T., Ramage, D., Amin, N., Schwikowski, B., Ideker, T., Cytoscape: a software environment for integrated models of biomolecular interaction networks. *Genome Res* 2003, *13*, 2498-2504.
[19] Ashburner, M., Ball, C. A., Blake, J. A., Botstein, D., Butler, H., Cherry, J. M., Davis, A. P., Dolinski, K., Dwight, S. S., Eppig, J. T., Harris, M. A., Hill, D. P., Issel-Tarver, L., Kasarskis, A., Lewis, S., Matese, J. C., Richardson, J. E., Ringwald, M., Rubin, G. M., Sherlock, G., Gene ontology: tool for the unification of biology. The Gene Ontology Consortium. *Nat Genet* 2000, *25*, 25-29.